

1. Oleksandr SAVCHENKO, 2. Huthaifa A. AL_ISSA, 3. Oleksandr MIROSHNYK, 4. Irina TRUNOVA,
5. Oleksandr Moroz, 6. Oleksandr KOZLOVSKYI, 7. Andriy VOLOBUYEV, 8. Dmytro YERMAK,
9. Taras SHCHUR, 10. Serhii STEPENKO, 11. Hristo Ivanov BELOEV, 12. Paweł KIELBASA

ORCID: 1. 0000-0002-6401-0852; 2. 0000-0002-8276-4906; 3. 0000-0002-6144-7573; 4. 0000-0001-7510-4291;
5. 0000-0002-8520-9211; 6. 0000-0001-6885-5994; 7. 0009-0001-1452-9285; 8. 0009-0008-1603-6338;
9. 0000-0003-0205-032X, 10. 0000-0001-7702-6776, 11. 0000-0002-8644-2947, 12. 0000-0003-0249-8626



DOI: 10.15199/48.2025.04.09

SolarM2P: map-to-point deep neural network for post-processing of numerical weather prediction-based solar irradiance forecasts

SolarM2P: głęboka sieć neuronowa typu mapa-punkt do przetwarzania końcowego numerycznych prognoz pogody opartych na natężeniu promieniowania słonecznego

Abstract: In this paper, we propose the SolarM2P deep convolutional neural network that implements a map-to-point approach for post-processing solar irradiance predictions based on Numerical Weather Prediction (NWP) models. The training and testing of the neural network were carried out on the archival data of solar irradiance forecasts of the Global Forecast System (GFS) for 2015-2023 for a part of the northeastern region of Ukraine. It is shown that the relative root mean square error (rRMSE) decreases from 40.4% for the best of the basic post-processing methods to 33.8% for the developed approach.

Streszczenie: W tym artykule zaproponowano głęboką splotową sieć neuronową SolarM2P, która implementuje podejście od mapy do punktu do postprocessingu prognoz natężenia promieniowania słonecznego w oparciu o modele numerycznych prognoz pogody (NWP). Uczenie i testowanie sieci neuronowej przeprowadzono na danych archiwalnych prognoz natężenia promieniowania słonecznego Globalnego Systemu Prognoz (GFS) na lata 2015-2023 dla części północno-wschodniego regionu Ukrainy. Pokazano, że względny błąd średniokwadratowy (rRMSE) zmniejsza się z 40,4% dla najlepszych podstawowych metod postprocessingu do 33,8% dla opracowanego podejścia.

Keywords: model output statistics; numerical weather prediction; solar irradiance forecasting.

Słowa kluczowe: statystyki wyjściowe modelu; numeryczne prognozowanie pogody; prognozowanie natężenia promieniowania słonecznego.

Introduction

Today, a large number of approaches have been developed to predict the power of solar power plants. Many of them use the solar radiation forecasting as a basis. A fairly broad overview of these approaches is given in [1]. For the purposes of long-range forecasting, physical methods based on Numerical Weather Prediction (NWP) models are the most appropriate. Despite the progress which was made in recent decades in long-term NWP based forecasting of solar irradiance, the accuracy of the forecasts remains relatively low. There is great potential in the development of post-processing approaches for NWP model prediction results. These approaches, traditionally referred to as model output statistics (MOS), have been actively developed for a long time [2-5]. Recently, for processing the results of NWP models, the modern methods based on machine learning and deep learning (deep neural networks) have been widely used [6, 7]. For example, [8] proposes several variants of deep neural networks for post-processing the results of the air temperature forecast, which is the output of the NWP model. However, this approach, in contrast to the one proposed by us, is more applicable for map-to-map converting. A number of other solar irradiance predicting approaches using deep neural networks employ sky images as input [9, 10] and they are therefore limited to a forecast horizon up to several hours ahead. A number of forecasting approaches based on deep neural networks have also been proposed that use time series of solar irradiance [11, 12], and in some cases, other meteorological parameters [13]. However, these approaches do not take into account the influence of the spatial distribution of predictors on the forecast.

In this article, we propose a map-to-point deep learning approach and a SolarM2P neural network architecture for post-processing of solar irradiance predictions made by NWP models. The suggested approach makes it possible to improve a number of indicators of forecast accuracy at a certain geographical point and at the same time can increase the temporal resolution.

Data

In the present article, the proposed deep learning approach was tested on the forecast data of the Global Forecasting System (GFS) developed by the US National Center for Environmental Prediction (NCEP) [14]. The studies used archival forecast data from 2015 to 2023 including. In this article, the value of prediction is Global Horizontal Irradiance (GHI). The data were taken for the forecast horizon up to 48 hours from the moment the model was launched. The result of the GFS forecast is presented with a spatial resolution of 0.25 degrees on a global grid of latitude and longitude. In our research, we used forecast data for 25 geographic points forming a rectangle with a central point with coordinates 49.75N, 36.0E, which is located in the vicinity of the town of Merefa, Kharkiv region, Ukraine. This point, for which the forecast of solar irradiance is refined, is referred to as the point of interest (POI) in the text. The location on the map of the Kharkiv region of the points for which the forecast data of the GFS model were used is shown in Fig. 1.

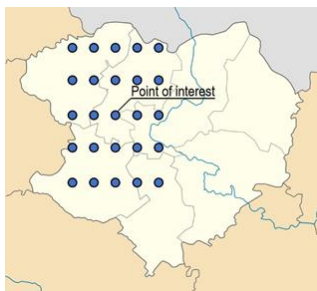


Fig. 1. Location of points on the map of Kharkiv region (Ukraine), for which the forecast data of the GFS model were used.

The data of direct measurements at hydrometeorological stations are most often used as actual solar irradiance data. However, for the territory of Ukraine, such data are limited and available only for some geographical points. There is also another approach to estimating the actual solar irradiance at a certain geographical point, which is based on the use of satellite images of the atmosphere [15]. This approach was used in the present work. We used solar irradiance data from the Copernicus Atmosphere Monitoring Service (CAMS) [16] as actual data. Throughout the rest of this article, we use the notation “satellite” for these data.

To apply the traditional method of increasing the temporal resolution of the solar irradiance forecast, which was used in this work as a baseline for evaluating the effectiveness of the proposed approach, information on the solar irradiance value for the case of a clear sky is required. In our study, we used the Ineichen and Perez clear sky model [17]. The monthly values of Linke’s turbidity were used. The clear sky data were generated using the python *pvl* library. In addition, with the help of this library, the zenith angle of the sun was obtained.

Benchmark methods

To evaluate the effectiveness of the proposed deep learning approach, in this article we also considered the basic methods for processing forecast results mentioned in a number of sources [3], [5]. The mentioned methods were used as a benchmark. Actually, they do not apply to MOS methods and only allow increasing the time resolution of the GFS model forecast to the required value of 1 hour. The following basic approaches for post-processing of the GFS model forecasts were considered:

1. A simplified approach based on the constancy of solar irradiance for each 3-hour period (the approach is denoted as “3h_const”).
2. An approach that uses direct linear interpolation of solar irradiance (the approach is denoted as “dir_inter”).
3. An approach in which the clear sky coefficient was assumed to be constant for each 3 hours (an approach denoted as “kt_const”).
4. An approach that uses linear interpolation of the clear sky coefficient (the approach is denoted as “kt_inter”).

In the first simplified approach, solar irradiance was assumed to be constant for each 3 hours and equal to the average value for this period, obtained from the GFS model.

In the second approach, direct linear interpolation of average 3-hour values is used to obtain 1-hour solar irradiance values.

The third approach involves the use of the clear sky coefficient which is calculated from the expression [3]:

$$(1) \quad k_t = I_t / I_{cs\ t}$$

where: I_t , $I_{cs\ t}$ – respectively denote the actual and clear sky value of GHI for hour t .

According to this approach, the value of the average clear sky coefficient for each of the 3-hour intervals k_{3h} is first calculated. Further, based on the assumption that this coefficient is constant throughout each of the intervals, the average values of solar irradiance for each hour within the interval were calculated using the expression $I_t = k_{3h} I_{cs\ t}$, where $I_{cs\ t}$ is the 1-hour average GHI value for hour t for clear sky conditions.

According to the fourth approach, after determining the average clear sky coefficient k_{3h} for each of the 3-hour intervals, its linear interpolation is carried out, which allows for obtaining coefficient values for each hour k_{1h} . Further, by analogy with the previous approach, the values of solar irradiance for each hour are determined.

Proposed deep learning approach for post-processing NWP based predictions

Some of the first deep neural networks that revolutionized computer vision tasks were AlexNet [18], VGGNet [19] and a number of others. Over the past decade, such CNNs have proven to be highly effective. They showed especially high performance in image processing tasks. The input of such a neural network is usually a 3-D pixel intensity tensor $m \times n \times c$, where m is the image height, n is its width, and c is the number of channels ($c = 3$ for color images). CNNs can be used both in classification problems [20] and in regression problems [21].

There is a direct analogy between the information obtained from the output of NWP models and the images processed by deep CNNs. In the case of the NWP output, we also have a 3-D tensor the elements of which are the value of a certain meteorological parameter, such as solar irradiance. The first and second dimensions of the mentioned tensor correspond to latitude and longitude, whereas as the third dimension (the number of input channels c_{in}) we can use the time slices of the NWP model prediction. Thus, we can build a deep CNN and enable it to learn complex spatiotemporal patterns in the data received from the NWP model and, as a result, improve prediction accuracy. In solar energy applications, we are usually interested in predicting the value of solar irradiance at a certain point, therefore, in this article, we considered a $1 \times 1 \times c_{out}$ tensor as the output of such a neural network. Such a neural network architecture implements the map-to-point approach.

Due to the features of CNN, the number of channels c_{out} in the output tensor can in principle be arbitrary and does not depend on the number of input channels c_{in} . Thus, we can arbitrarily adjust the temporal resolution of the data, for example, upwards. As already noted in this article, the proposed deep learning approach was tested on the output of the GFS model, which is a forecast of solar irradiance with time averaging over every 3 hours. We used a forecast horizon of up to 48 hours from the start of the model. Thus, the number of input channels is $c_{in} = 16$. In solar energy applications, a time resolution of 1 hour is currently acceptable. With a constant forecast horizon of up to 48 hours, the number of channels at the output of the neural network should be $c_{out} = 48$.

The choice of the size $m \times n$ of the initial data map, based on which the forecast of solar irradiance at the POI is carried out, was made based on an analysis of the literature. Thus, [3] found that the greatest increase in forecast accuracy is obtained by simply averaging the output of the ECMWF model on a 4×4 grid. A similar conclusion was obtained [22] for the GFS model at the same spatial resolution. For reasons of symmetry, we chose the size of the data map as 5×5 , with the POI placed in the center. Given the spatial resolution of the GFS model

of 0.25 degrees, this field corresponds to the size of the region of approximately 100×100 km. It should be noted that in the case of processing the output of the GFS model using CNN, a more sophisticated approach takes place, since the data at different points are combined using different weights obtained by training the neural network.

The architecture of the proposed SolarM2P neural network which is based on convolutional layers, is shown in Fig. 2. In essence, this model is a regression model, at the output of which 48 continuous values are predicted - GHI for each of the 48 hours within the forecast horizon.

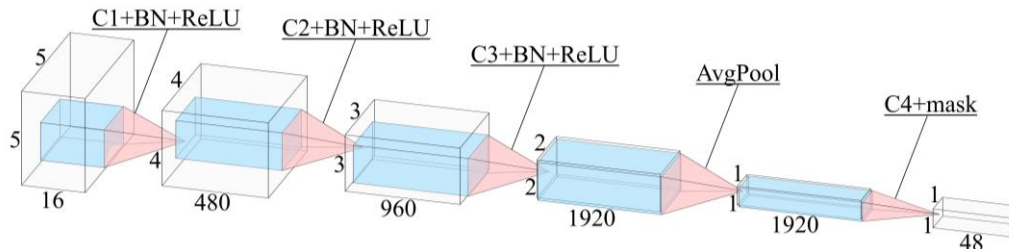


Fig. 2. The structure of the proposed SolarM2P neural network for post-processing the solar irradiance forecasts of NWP models. The network implements a map-to-point approach. The figure indicates: C1...C4 – 2D convolution operations, BN – batch normalization operation, ReLU – activation function, AvgPool – averaging pooling operation, mask – mask application (see explanation further in the article). The numbers indicate the sizes of the tensors after the various layers of the network.

As it is known, training a neural network consists in finding such values of weights in its layers that lead to the minimum value of the loss function. The average sum of squared errors, which is most often used for regression problems [23, 24], was used as a loss function:

$$(3) \quad MSE = \frac{1}{N} \sum_{i=1}^N (I_{out\ i} - I_{ground\ i})^2$$

where: $I_{out\ i}$, $I_{ground\ i}$ – respectively, the value of the i -th element of the output tensor of the neural network and the ground true value, N – the number of elements over which the averaging is carried out.

In total, there were 6512 days of forecasts in the dataset (for the period 2015-2023, there were two forecasts for each day). The data were randomly divided into three parts: data for training (about 70% of all data), data for validation, according to which the hyperparameters of the model were selected (about 15% of all data), data for testing (about 15% of all data). This sampling method ensured data consistency in the training, validation, and test data sets. The check showed that in all datasets, different periods of the year were presented in the same way, which makes it possible to obtain a more robust post-processing method.

The training was carried out by the method of error backpropagation. For optimization batch gradient descent was used with $batch_size = 32$. To increase the speed of learning, z-scaling of the data was applied based on the mean and standard deviation. Such normalization was carried out for input and output data, separately for each channel.

After training, the weights in the layers of the neural network remain unchanged. The use of a neural network for post-processing of solar irradiance forecast data with a prediction horizon of 48 hours consists in feeding a tensor of the appropriate dimension, which is the output of the GFS model, to CNNs input. The neural network performs a mapping of the form (2), the result of which is an updated forecast at the POI.

Thus, the neural network performs a nonlinear transformation of the form:

$$(2) \quad I_{out} = F(I_{in})$$

where: I_{in} – the input tensor, which is a set of solar irradiance prediction maps made by the NWP model, I_{out} – the output tensor, which is an updated forecast of solar irradiance at the POI.

All the approaches considered in this article, due to the imperfection of the models used, can lead to inadequate forecasts. For example, forecasts of solar irradiance $I_t < 0$ with small absolute values in the morning and evening hours. Therefore, for all approaches, we used a set of corrective rules of the form:

$$(4) \quad I_t = \begin{cases} 0 & \text{if } I_t < 0 \\ 1.25I_{cs\ t} & \text{if } I_t > 1.25I_{cs\ t} \end{cases}$$

It should also be emphasized that the neural network should be used to post-process the GFS model predictions only at the POI for which it was trained (or very close to it). A different model must be trained and used to post-process a forecast at a different geographic location for obtaining similar accuracy scores.

The baseline from which many of the solar irradiance forecast accuracy metrics are calculated is the forecast error for a particular hour t :

$$(5) \quad e_t = I_t - I_{ground\ t}$$

where: I_t , $I_{ground\ t}$ – respectively, the predicted and true values of solar irradiance for hour t .

An important predictive accuracy metric used in this article is the mean bias error:

$$(6) \quad MBE = \frac{1}{T} \sum_{t=1}^T e_t$$

where: T – the length of the forecast period.

The MBE can be used to estimate the systematic shift of the forecast up or down.

As noted in a number of sources [2], [3], for solar power applications, the most relevant is the use of the standard error of the forecast, which imposes a larger penalty for large deviations in the forecast:

$$(7) \quad RMSE = \sqrt{\frac{1}{T} \sum_{t=1}^T e_t^2}$$

Also, the accuracy of the forecast can be further evaluated using the mean absolute error, which is more applicable for applications in which the linear dependence of the penalty on the magnitude of the error is typical:

$$(8) \quad MAE = \frac{1}{T} \sum_{t=1}^T |e_t|.$$

Another predictive accuracy metric used is Pearson's linear correlation coefficient between predicted and actual values of solar irradiance:

$$(9) \quad \rho = \frac{cov(I_t, I_{ground \ t})}{\sigma_{I_t} \sigma_{I_{ground \ t}}}$$

where: $cov(I_t, I_{ground \ t})$ – the covariance of predicted and actual values of solar irradiance, σ_{I_t} , $\sigma_{I_{ground \ t}}$ are the standard deviation of predicted and actual values of solar irradiance, respectively.

Relative variants of MBE, RMSE and MAE make it possible to compare the accuracy of forecasts for conditions with different average solar irradiance levels:

$$(10) \quad rMBE = \frac{MBE}{I_{ground \ mean}} 100, \%$$

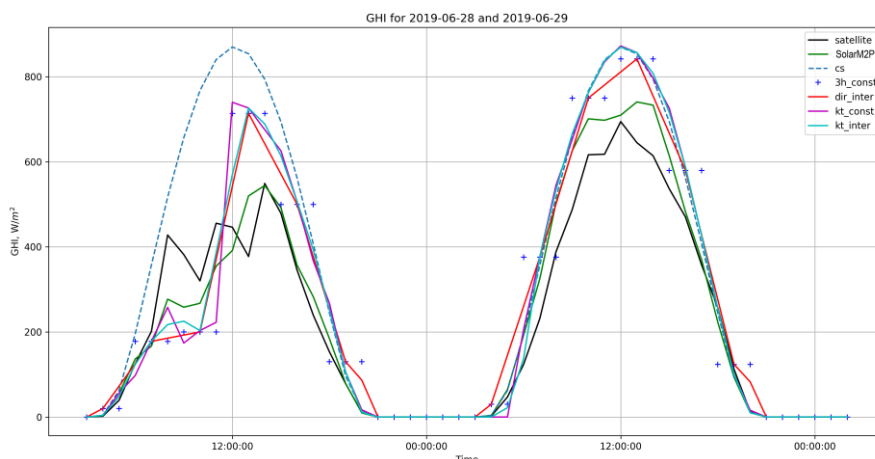


Fig.3. Plot of solar irradiance forecasts for two summer days (June 28 and 29, 2019).

Table 1. Accuracy metrics for the basic and proposed approaches for post-processing the solar irradiance forecast of the GFS model

Approach	Metric						
	RMSE (W/m ²)	rRMSE (%)	MBE (W/m ²)	rMBE (%)	MAE (W/m ²)	rMAE (%)	ρ
3h_const	126.33	49.18	31.54	12.28	89.55	34.86	0.88
dir_inter	103.74	40.39	30.03	11.69	70.06	27.27	0.92
kt_const	110.03	42.83	33.22	12.93	63.4	24.68	0.92
kt_inter	106.68	41.53	32.38	12.61	61.1	23.79	0.92
SolarM2P	86.69	33.75	-0.38	-0.15	53.96	21.01	0.94

$$(11) \quad rRMSE = \frac{RMSE}{I_{ground \ mean}} 100, \%$$

$$(12) \quad rMAE = \frac{MAE}{I_{ground \ mean}} 100, \%$$

where: $I_{ground \ mean}$ – the average value of the actual solar irradiance in the entire dataset.

The above metrics were calculated for the POI (49.75N, 36.0E) only for hours when solar irradiance for clear weather conditions $I_{cs \ t} > 0$ (night hours were not taken into account). Also, we did not introduce a limitation on the zenith angle of the sun, as is sometimes done in similar calculations [5].

Results and discussion

As an example, Fig. 3 shows solar irradiance forecasts for two summer days. The forecasts were obtained using various post-processing methods. The same figure shows actual GHI values and values for clear sky conditions. An analysis of such graphs showed that the weather patterns studied by the neural network allow it to more adequately respond to changes in the level of solar irradiance, both downward and upward. However, as expected, sometimes the neural network is unable to predict sudden changes in solar irradiance.

The trained neural network was used to post-process the results of the GFS model prediction from the test dataset (this approach is referred to as “SolarM2P” in the text of the work). The test set included a total of 976 days of forecasts. For exactly the same test set, the traditional post-processing methods (described in this article in “Benchmark methods” section) were applied, which were used as baselines. The results of calculating the accuracy metrics of these approaches are shown in Table 1.

As it can be seen from Table 1, the proposed deep learning approach improves all the considered forecast accuracy metrics. The improvement of one of the main metrics for solar power applications, $rRMSE$, is especially noticeable, which, compared with the best of the basic post-processing approaches, decreases in absolute terms by almost 7% (in relative terms, the decrease is 16% to the initial value). The post-processing approach proposed by this work obtained a value of 33.75% to $rRMSE$ metric. In other words, the proposed method provides better results than the ones shown in [4] (40.5%) and [5] (35.7%) in terms of forecast post-processing methods. A similar and significant improvement has been also noticed in the MBE value, which tends to zero (i.e., a forecasted parameter achieved values that are slightly closer to the real values observed in a real physical parameter). It suggests that after the proposed post-processing there is practically no

systematic forecast shift. $rMAE$ and correlation coefficient ρ are also improved, although not as much. It should be noted that in the case of applying the proposed post-processing method in regions with sharply changing weather conditions, some deterioration of forecast accuracy metrics is possible in comparison with the values given in the Table 1. However, this situation is typical for any forecasting or post-processing method.

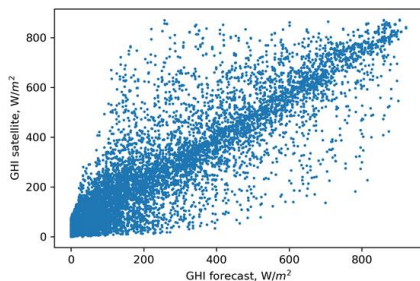


Fig. 4. Scatter plot of predicted (GHI forecast) and actual (GHI satellite) solar irradiance values for the POI. The predicted values are obtained using the proposed approach.

Figure 4 shows a scatter plot of predicted and actual values of solar irradiance which can be used to visually assess the degree of linear relationship between these values. As can be seen, the prediction of the GFS model with post-processing based on the proposed approach demonstrates a good agreement with the actual values of solar irradiance. Although it is possible to notice a high number of spread points (compared to the diagonal ideal reference), such an effect is considered typical for long-term forecasting methods due to the divergence between predicted and real values of a physical parameter. The longer the forecasting horizon, the wider the spread points get. For example, in [5] a rather lower correlation coefficient of about 0.7 was obtained.

Conclusion

This work proposed a map-to-point approach and SolarM2P neural network for post-processing of solar irradiance predictions made by NWP models. The evaluation of the proposed approach was carried out on a test set of GFS model forecasts with an equivalent duration

of almost 3 years and various weather conditions, which allows us to speak about the adequacy of the obtained accuracy metrics. As a result of the research, it was found that the proposed approach can significantly improve a number of the most common indicators of the accuracy of solar irradiance forecasts. At the same time, a feature of the proposed approach is also the possibility of an arbitrary increase in the temporal resolution of the forecast.

Authors: assoc. prof. Oleksandr Savchenko, State Biotechnological University, Department of Power Supply and Energy Management, Kharkiv, Alchevskiyh 44, 61002 Kharkiv, Ukraine, E-mail: savoa@btu.kharkiv.ua; assoc. prof. Huthaifa A. Al_Issa, Al Balqa Applied University, Department of Electrical and Electronics Engineering, Al Salt, 19117, Jordan, E-mail: h.alissa@bau.edu.jo; prof. dr hab. inż. Oleksandr Miroshnyk, State Biotechnological University, Department of Power Supply and Energy Management, Kharkiv, Alchevskiyh 44, 61002 Kharkiv, Ukraine, E-mail: omiroshnyk@btu.kharkiv.ua; assoc. prof. Irina Trunova, State Biotechnological University, Department of Power Supply and Energy Management, Kharkiv, Alchevskiyh 44, 61002 Kharkiv, Ukraine, E-mail: trunova_iryina@btu.kharkiv.ua; prof. dr hab. inż. Oleksandr Moroz State Biotechnological University, Department of Power Supply and Energy Management, Kharkiv, Alchevskiyh 44, 61002 Kharkiv, Ukraine, E-mail: moroz.an@btu.kharkiv.ua; assoc. prof. Oleksandr Kozlovskiy, Central Ukrainian National Technical University, Department of Electrical Systems and Energy Management, pr. Universytetskyi 8, 25006, Kropyvnytskyi, Ukraine. E-mail: kozlovskiyoa@gmail.com; PhD, Andriy Volobuyev, State Biotechnological University, Department of Power Supply and Energy Management, Kharkiv, Alchevskiyh 44, 61002 Kharkiv, Ukraine, E-mail: andreyvolobuev7777@gmail.com; PhD, Dmytro Yermak State Biotechnological University, Department of Power Supply and Energy Management, Kharkiv, Alchevskiyh 44, 61002 Kharkiv, Ukraine, E-mail: golf9292ua@gmail.com; Phd, Taras Shchur, Cyclone Manufacturing Inc, Mississauga, Ontario, Canada, E-mail: shchurtg@gmail.com; Department of Electrical Engineering, Information and Measurement Technologies, Chernihiv Polytechnic National University, Chernihiv 14030, Ukraine, E-mail: serhii.stepenko@stu.cn.ua, prof Hristo Ivanov Beloev, University of Ruse, 8 Studentska str., POB 7017, Ruse, Bulgaria, hbeloev@uni-ruse.bg., Paweł Kielbasa Associate Professor, University of Agriculture in Krakow, Faculty of Production and Power Engineering, Balicka Av. 116B, 30-149 Krakow, E-mail: pawel.kielbasa@urk.edu.pl

REFERENCES

- [1] Ahmed R., Sreeram V., et al., A review and evaluation of the state-of-the-art in PV solar power forecasting: Techniques and optimization. *Renew Sustain Energy Rev*, 124, (2020), 109792. doi: 10.1016/J.RSER.2020.109792
- [2] Perez R., Lorenz E., et al., Comparison of numerical weather prediction solar irradiance forecasts in the US, Canada and Europe. *Sol Energy*, 94, (2013), 305-326. doi: 10.1016/J.SOLENER.2013.05.005
- [3] Lorenz E., Hurka J., et al., Irradiance Forecasting for the Power Prediction of Grid-Connected Photovoltaic Systems. *IEEE J Sel Top Appl Earth Obs Remote Sens*, 2, (2009), 2-10
- [4] Qawaqzeh M., Al_Issa H., Buinyi R., Bezruchko V., Dikhtyaruk I., Miroshnyk O., Nitsenko V. The assess reduction of the expected energy not-supplied to consumers in medium voltage distribution systems after installing a sectionalizer in optimal place. *Sustain. Energy, Grids and Networks*, 34, (2023), 101035. doi: 10.1016/j.segan.2023.101035
- [5] Verbois H., Huva R., Rusydi A., Walsh W. Solar irradiance forecasting in the tropics using numerical weather prediction and statistical learning. *Sol Energy*, 162, (2018), 265-77. doi: 10.1016/J.SOLENER.2018.01.007
- [6] Dewitte S., Cornelis J.P., Müller R., Munteanu A. Artificial Intelligence Revolutionises Weather Forecast, Climate Monitoring and Decadal Prediction. *Remote Sens*, (2021), 13. doi: 10.3390/rs13163209
- [7] Savchenko O., Miroshnyk O., Moroz O., Trunova I., Sereda A., Dudnikov S., Kozlovskiy O., Buinyi R., Halko S. Improving the efficiency of solar power plants based on forecasting the intensity of solar radiation using artificial neural networks. *2021 IEEE 2nd KhPI Week on Advanced Technology (KhPIWeek)*. (2021), 137-140. doi: 10.1109/KhPIWeek53812.2021.9570009.
- [8] Chen K., Wang P., Yang X., Zhang N., Wang D. A Model Output Deep Learning Method for Grid Temperature Forecasts in Tianjin Area. *Appl Sci*, (2020), 10. doi: 10.3390/app10175808
- [9] Feng C., Zhang J., Zhang W., Hodge B-M. Convolutional neural networks for intra-hour solar forecasting based on sky image sequences. *Appl Energy*, 310, (2022), 118438. doi: 10.1016/j.apenergy.2021.118438
- [10] Siddiqui TA, Bharadwaj S, Kalyanaraman S. A Deep Learning Approach to Solar-Irradiance Forecasting in Sky-Videos. *2019 IEEE Winter Conf. Appl. Comput. Vis.*, (2019), 2166-74. doi: 10.1109/WACV.2019.00234.
- [11] Dairi A, Harrou F, Sun Y. A deep attention-driven model to forecast solar irradiance. *2021 IEEE 19th Int. Conf. Ind. Informatics*, (2021), 1-6. doi: 10.1109/INDIN45523.2021.9557405

- [12] Qawaqzeh M., Miroshnyk O., Shchur T., Kasner R., Idzikowski A., Kruszelnicka W., Tomporowski A., Baldowska-Witos P., Flizikowski J., Zawada M., et al. Research of Emergency Modes of Wind Power Plants Using Computer Simulation. *Energies*, 14, (2021), 4780. doi: 10.3390/en14164780
- [13] Blazakis K, Katsigiannis Y, Stavrakakis G. One-Day-Ahead Solar Irradiation and Windspeed Forecasting with Advanced Deep Learning Techniques. *Energies*, (2022), 15. doi: 10.3390/en15124361
- [14] Szafraniec A., Halko S., Miroshnyk O., Figura R., Zharkov A., Vershkov O. Magnetic field parameters mathematical modelling of windelectric heater. *Przegląd Elektrotechniczny*, 97 (2021), 8, 36-41. doi: 10.15199/48.2021.08.07
- [15] Palmer D., Koubli E., et al., Satellite or ground-based measurements for production of site specific hourly irradiance data: Which is most accurate and where? *Sol Energy*, 165, (2018), 240-55. doi: 10.1016/J.SOLENER.2018.03.029
- [16] Komada P., Trunova I., Miroshnyk O., Savchenko O., Shchur T. The incentive scheme for maintaining or improving power supply quality. *Przegląd Elektrotechniczny*, 95, (2019), 5, 79-82. doi: 10.15199/48.2019.05.20
- [17] Ineichen P., Perez R. A New Airmass Independent Formulation for the Linke Turbidity Coefficient. *Sol Energy*, 73, (2002), 3, 151-157. [https://doi.org/10.1016/S0038-092X\(02\)00045-2](https://doi.org/10.1016/S0038-092X(02)00045-2)
- [18] Krizhevsky A., Sutskever I., Hinton G.E. ImageNet Classification with Deep Convolutional Neural Networks. *Communications of the ACM*, 60, (2017), 6, 84-90. <https://doi.org/10.1145/3065386>
- [19] Halko S., Suprun O., Miroshnyk O., Influence of Temperature on Energy Performance Indicators of Hybrid Solar Panels Using Cylindrical Cogeneration Photovoltaic Modules. *2021 IEEE 2nd KhPI Week on Advanced Technology (KhPIWeek)*, (2021), 132-136. doi: 10.1109/KhPIWeek53812.2021.9569975
- [20] He K., Zhang X., Ren S., Sun J. Deep Residual Learning for Image Recognition. *2016 IEEE Conference on Computer Vision and Pattern Recognition (CVPR)*, Las Vegas, NV, USA, (2016), 770-778, doi: 10.1109/CVPR.2016.90
- [21] Lathuilière S., Mesejo P., et al., A Comprehensive Analysis of Deep Regression. *IEEE Trans Pattern Anal Mach Intell*, 42, (2020), 2065-2081. doi: 10.1109/TPAMI.2019.2910523
- [22] Mathiesen P, Kleissl J. Evaluation of numerical weather prediction for intra-day solar forecasting in the continental United States. *Sol Energy*, 85, (2011), 967-977. doi: 10.1016/j.solener.2011.02.013
- [23] Khasawneh A., Qawaqzeh M., Kuchanskyy V., Rubanenko O., Miroshnyk O., Shchur T., Drechny M. Optimal Determination Method of the Transposition Steps of An Extra-High Voltage Power Transmission Line. *Energies*, 14, (2021), 20, 6791. doi: 10.3390/en14206791
- [24] Chollet F. Deep Learning with Python. 1st ed. USA: Manning Publications Co. (2017).